

Dual Modulation of Human P-Glycoprotein and ABCG2 with Prodrug Dimers of the Atypical Antipsychotic Agent Paliperidone in a Model of the Blood–Brain Barrier

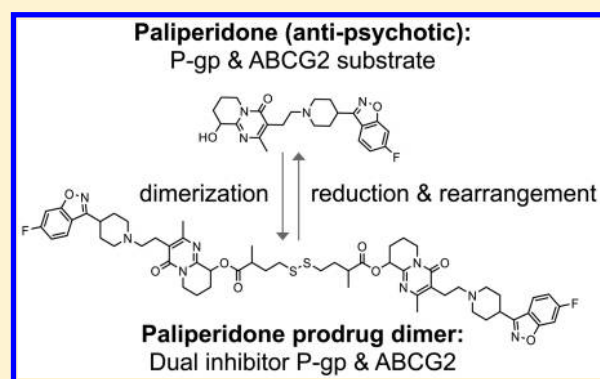
Kelsey Bohn, Allison Lange, Jean Chmielewski,* and Christine A. Hrycyna*[✉]

Department of Chemistry and Institute for Integrative Neuroscience, Purdue University, West Lafayette, Indiana 47907, United States

Supporting Information

ABSTRACT: Many atypical antipsychotic drugs currently prescribed for the treatment of schizophrenia have limited brain penetration due to the efflux activity of ATP-binding cassette (ABC) transporters at the blood–brain barrier (BBB), including P-glycoprotein (P-gp) and ABCG2. Herein, we describe the design and synthesis of the first class of homodimeric prodrug dual inhibitors of P-gp and ABCG2. These inhibitors are based on the structure of the atypical antipsychotic drug paliperidone (Pal), a transport substrate for both transporters. We synthesized and characterized a small library of homodimeric bivalent Pal inhibitors that contain a variety of tethers joining the two monomers via ester linkages. The majority of our compounds were low micromolar to sub-micromolar inhibitors of both P-gp and ABCG2 in cells overexpressing these transporters and in immortalized human hCMEC/D3 cells that are derived from the BBB. Our most potent dual inhibitor also contained an internal disulfide bond in the tether (Pal-8SS) that allowed for rapid reversion to monomer in the presence of reducing agents or plasma esterases. To increase stability against these esterases, we further engineered Pal-8SS to contain two hindering methyl groups alpha to the carbonyl of the ester moiety within the tether. The resulting dimer, Pal-8SSMe, was also a potent dual inhibitor that remained susceptible to reducing conditions but was more resistant to breakdown in human plasma. Importantly, Pal-8SSMe both accumulated and subsequently reverted to the therapeutic Pal monomer in the reducing environment of BBB cells. Thus, these molecules serve two purposes, acting as both inhibitors of P-gp and ABCG2 at the BBB and as prodrugs, effectively delivering therapies to the brain that would otherwise be precluded.

KEYWORDS: ABC transporter, blood–brain barrier, atypical antipsychotic, drug transport



INTRODUCTION

The World Health Organization (WHO)¹ estimates that more than 21 million people worldwide are affected by schizophrenia, ranking it as one of the most disabling mental illnesses.¹ Atypical antipsychotics are currently the most prescribed treatments for schizophrenia.^{2,3} Among this class of drugs, paliperidone (Pal, 9-hydroxyrisperidone, Invega) and its long-acting injectable formulations (Invega Sustenna and Invega Trinza, paliperidone palmitate) are some of the most widely used.^{4,5} Furthermore, Pal, which is the active metabolite of risperidone, is also the only treatment currently FDA approved as a monotherapy for schizoaffective disorder, which presents as a combination of symptoms relating to both schizophrenia and mood disorders.⁵

To be effective, antipsychotic drug therapies need to reach the brain in sufficient amounts. However, access to the brain can be limited by the blood–brain barrier (BBB). The BBB is reported to exclude 100% of large-molecule and 98% of small-molecule drugs due in large part to tight junctions between adjacent brain endothelial cells and the efflux activity of several

ATP-binding cassette (ABC) transporters.^{6–8} To penetrate the BBB and reach therapeutically relevant concentrations, combination therapies or higher doses are administered, which can contribute to the wide array of serious side effects seen with antipsychotics such as extreme weight gain, movement disorders, and cardiac irregularities.^{2,9,10}

Of the ABC transporters expressed at the BBB, P-glycoprotein (P-gp) is the most abundant and has been shown to actively efflux therapeutic agents including antipsychotic therapies from the brain both *in vitro* and *in vivo*.^{11–15} Another ABC transporter at the BBB is ABCG2, which has significant substrate redundancy with P-gp, while also having its own distinct subset of substrates.^{16–19} These overlapping substrate specificities enhance the protective function of the BBB. *In vitro*, Pal was shown to be a substrate of human and

Received: November 17, 2016

Revised: January 26, 2017

Accepted: March 6, 2017

Published: March 6, 2017

mouse P-gp using a Transwell assay that measures drug transport across cell monolayers.²⁰ *In vivo*, marked increases in the brain concentration of Pal in P-gp knockout mice as compared to wild-type mice were observed, suggesting that Pal is excluded from the brain due to P-gp transport.^{21,22} Until our present study, Pal had not been evaluated as a direct transport substrate for ABCG2.

In some cases, substrates of ABC transporters act as inhibitors at higher concentrations.^{23–25} In this regard, Pal has been reported to weakly inhibit P-gp mediated transport of the fluorescent substrate rhodamine 123 (R123) in cells overexpressing P-gp at concentrations >100 μM .²⁶ In addition, efflux of the fluorescent substrate mitoxantrone by ABCG2 was inhibited by Pal in cells overexpressing the transporter, with an IC_{50} of ~ 50 μM .²⁷ Taken together, these results suggest that Pal can act as an inhibitor of P-gp and ABCG2 at higher concentrations.

Both P-gp and ABCG2 are proposed to have multiple, spatially distinct binding sites that recognize a wide variety of substrates.^{23,25,28–39} We and others have taken advantage of these multiple sites in the design of bivalent agents as potent inhibitors of P-gp.^{40–47} In contrast to the large number of compounds reported to be substrates to both P-gp and ABCG2, a relatively low number of dual P-gp/ABCG2 inhibitors have been identified. Current dual inhibitors of P-gp and ABCG2 include elacridar (GF120918), bifendate-chalcone hybrids, biricodar (VX-710), sunitinib, and other tyrosine kinase inhibitors (TKIs).^{48–52} Dual inhibitors of P-gp and ABCG2 could be beneficial for increasing the central nervous system (CNS) penetration of therapies that are substrates of both transporters. However, these dual inhibitors often demonstrate lower potency against one of the transporters, necessitating the development of new agents.

Herein, we report the first homodimeric bivalent dual inhibitors of P-gp and ABCG2 that are active in both cell lines overexpressing each transporter and cells derived from the BBB. These inhibitors also act as prodrugs, reverting to the therapeutic monomeric species once across the blood–brain barrier. Thus, these dimers serve a dual role, both inhibiting P-gp and ABCG2 and effectively delivering therapies to the brain that would otherwise be precluded.

■ EXPERIMENTAL PROCEDURES

Materials. Pal was purchased from Avachem Scientific LLC (San Antonio, TX), Santa Cruz Biotechnology (Dallas, TX), and Boc Sciences (Shirley, NY). GF120918 was synthesized in our laboratory as previously described.⁴² Mitoxantrone was purchased from LKT Laboratories, Inc. (St. Paul, MN). R123, calcein-AM, Sf9 cells, and antibiotic–antimycotic were purchased from Invitrogen (Carlsbad, CA). Fetal bovine serum (FBS) was purchased from Atlanta Biologicals (Lawrenceville, GA). L-Glutamine, penicillin–streptomycin, and basal medium Eagle were purchased from Mediatech (Herdon, VA). [¹²⁵I]-IAAP was purchased from PerkinElmer (Waltham, MA). N-(3-(Dimethylamino)propyl)-N-ethylcarbodiimide (EDC) was purchased from AK Scientific (Union City, CA). Cultrex rat collagen I was obtained from Trevigen (Gaithersburg, MD). EBM-2 medium was purchased from Lonza (Visp, Switzerland). hCMEC/D3 cells were obtained under license from Institut National de la Santé et de la Recherche Médicale (INSERM, Paris, France). The C219 antibody was a generous gift from Dr. Michael M. Gottesman (National Cancer Institute, NIH, Bethesda, MD). The BXP21

antibody was obtained from Novus Biologicals (Littleton, CO). All other reagents and chemicals were purchased from either Sigma-Aldrich (St. Louis, MO) or Invitrogen (Carlsbad, CA).

Synthesis of Ester Linked Pal Dimers. Pal dimers were synthesized using the commercially available racemic mixture of Pal. All tethers were commercially available with the exception of 5,5'-disulfanediyldipentanoic acid, which was synthesized using previously reported methods.^{53,54} To a solution of diacid tether (0.04 mmol) in dry dichloromethane (1 mL) at 0 °C were added EDC (0.13 mmol), 4-dimethylaminopyridine (0.02 mmol), and DIEA (0.39 mmol). After stirring at 0 °C for 20 min, Pal (0.12 mmol) was added. The mixture was brought back to room temperature and stirred for 36 h protected from light. The solvent was removed *in vacuo*, and the dimers were purified to homogeneity by reverse phase HPLC using a C5 column (Phenomenex, Torrance, CA) with an eluent consisting of solvent A (water and 0.1% trifluoroacetic acid (TFA)) and solvent B (methanol with 0.1% TFA) with a gradient of 20–95% solvent B, a flow rate of 8 mL/min, and UV detection at 214 and 280 nm. The pure compounds (>95% by analytical HPLC) were characterized by ESI mass spectrometry. PalC2 [M + H]⁺: 935.0 calculated, 935.4 observed. PalC4 [M + H]⁺: 963.1 calculated, 963.2 observed. PalC6 [M + H]⁺: 991.1 calculated, 991.7 observed. PalC8 [M + H]⁺: 1019.2 calculated, 1019.4 observed. Pal-8SS [M + H]⁺: 1055.3 calculated, 1055.8 observed. PalC10 [M + H]⁺: 1047.2 calculated, 1047.4 observed. Pal-10SS [M + H]⁺: 1083.31 calculated, 1084.0 observed. PalC12 [M + H]⁺: 1075.3 calculated, 1076.2 observed. Pal-8SSMe [M + H]⁺: 1083.3 calculated, 1083.8 observed.

Synthesis of Carbamate Linked Pal Dimer. Pal (0.12 mmol) was dissolved in dry dichloromethane (1 mL). After stirring for 5 min at room temperature, 1,1'-carbonyldiimidazole (0.12 mmol) and DIEA (0.20 mmol) were added and stirred for 4 h at room temperature. Hexane 1,6-diamine (0.04 mmol) was added, and the reaction proceeded for 24 h at room temperature protected from light. Solvent was removed *in vacuo*, and dimer was purified from the reaction mixture using reverse phase HPLC using a C18 column (Phenomenex, Torrance, CA) with an eluent consisting of solvent A (water and 0.1% TFA) and solvent B (acetonitrile and 0.1% TFA) with a gradient of 30–95% solvent B, a flow rate of 10 mL/min, and UV detection at 214 and 280 nm. The pure compound (>95% by analytical HPLC) was characterized by ESI mass spectrometry. Pal-carbamate [M + H]⁺: 1021.2 calculated, 1021.0 observed.

Cell Culture. MCF-7 cells were maintained at 37 °C with 5% CO₂ in RPMI 1640 medium containing 2 mM L-glutamine, 10% fetal bovine serum, 50 units/mL of penicillin, and 50 $\mu\text{g}/\text{mL}$ of streptomycin.⁵⁵ MCF-7/DX1 cells were maintained as above with the addition of 1 μM doxorubicin.⁵⁶ MCF-7/FLV1000 cells were maintained as described above except with 1 μM flavopiridol.¹⁷ Sf9 cells were cultured at 27 °C in SF-900 II SFM medium supplemented with 0.5 \times antibiotic–antimycotic. hCMEC/D3 cells were cultured in EBM-2 medium supplemented with 5% fetal bovine serum, 1% penicillin–streptomycin, 1.4 μM hydrocortisone, 5 $\mu\text{g}/\text{mL}$ ascorbic acid, 1:100 dilution of chemically defined lipid concentrate, 10 mM HEPES, and 1 ng/mL basic fibroblast growth factor.⁵⁷ The culture flasks were coated with 0.1 mg/mL rat tail collagen for at least 1 h at 37 °C before use, and cells were incubated at 37 °C with 5% CO₂.

Expression of P-gp or ABCG2 in Insect Cells. Sf9 cells in 150 cm² flasks were infected with baculovirus (BV)-MDR1 or BV-ABCG2 at a multiplicity of infection of five.^{58,59}

Preparation of Crude Insect Cell Membranes. P-gp and ABCG2 overexpressing crude membrane extracts were prepared as previously described.⁵⁸ BV-MDR1 and BV-ABCG2 infected Sf9 cells were harvested 72 h after infection by centrifugation. The membrane pellet was resuspended in homogenization buffer containing 50 mM Tris (pH 7.5), 50 mM mannitol, 2 mM ethylene glycol tetraacetic acid (EGTA), 1 mM 4-(2-aminoethyl)benzenesulfonyl fluoride hydrochloride (AEBSEF), 2 mM dithiothreitol (DTT), and 1% aprotinin. The cells were incubated on ice for 40 min and then homogenized by 40 strokes with a Dounce homogenizer (pestle A and B). The nuclear debris was removed by centrifugation at 3000g for 10 min. Crude membranes were isolated by centrifugation of the supernatant at 100000g for 60 min at 4 °C and resuspended using blunt-end 18-, 20-, 22-, and 25-gauge needles sequentially in buffer (50 mM Tris, pH 7.5, 200 mM mannitol, 1 mM EGTA, 1 mM AEBSEF, 1 mM DTT, 1% aprotinin, and 10% glycerol). The membranes were stored at -80 °C. P-gp expression was confirmed by immunoblot with C219 primary antibody (1:4000) and HRP-conjugated goat-anti-mouse secondary antibody (1:4000). ABCG2 expression was confirmed by immunoblot with BXP21 primary antibody (1:2000) and HRP-conjugated goat-anti-mouse secondary antibody (1:4000).

Preparation of Mammalian Crude Membranes. Crude membrane extracts from mammalian cells were prepared as described previously.⁶⁰ The resuspended membranes were stored at -80 °C.

96-Well Plate Rapid Screen of P-gp Substrate Accumulation Assay. Assays were performed as described previously with modifications.⁶¹ MCF-7/DX1 cells (20,000 cells) were plated the night before in RPMI 1640 containing 2 mM L-glutamine, 10% fetal bovine serum, 50 units/mL of penicillin, and 50 µg/mL of streptomycin. On the day of the assay, the medium was removed and 150 µL of basal medium Eagle (BME) supplemented with 5% FBS cell culture medium containing 1 µM calcein-AM and increasing concentrations of inhibitor was added to each well. All compounds were dissolved in DMSO with the final concentration of DMSO at 2% to allow for testing of higher concentrations of inhibitor. The 96-well plate was incubated at 37 °C for 10 min. The medium was aspirated, and the plate was kept on ice. Fluorescence intensities were immediately read on a Spectrafluor Plus plate reader (TECAN Systems, San Jose, CA) with excitation/emission filters of 492 nm/535 nm. GF120918 (1 µM) was used as a positive control. The mean fluorescence values were used to calculate IC₅₀ values with GraphPad Prism 4.0.

Flow Cytometry Assays. Flow cytometry assays were performed as described previously with some modifications.⁶⁰ MCF-7/DX1 cells or hCMEC/D3 cells (125,000 cells) were incubated with R123 (0.5 µg/mL) or calcein-AM (0.5 µM). MCF-7/FLV1000 cells (125,000 cells) were incubated with mitoxantrone (20 µM). Fluorophore and increasing concentrations of inhibitors in BME supplemented with 5% FBS were added to the samples and incubated for 30 min (R123 and mitoxantrone) or 10 min (calcein-AM) at 37 °C. The cells were pelleted by centrifugation at 300g at 4 °C for 5 min, and the medium was removed. Samples with calcein-AM were stored on ice. The cells with R123 and mitoxantrone were subsequently resuspended in 1 mL of BME medium and the

compound of interest in increasing concentrations and incubated for an additional 30 min at 37 °C to allow for efflux. The medium was again removed after centrifugation, and the cells were kept on ice. Immediately before analysis, cells were resuspended in 350 µL of PBS (pH 7.4). Samples were analyzed using a FACSCalibur flow cytometer with a 488 nm argon laser and a 670 nm band-pass filter (FL3) for mitoxantrone and a 585/42 band-pass filter (FL1) for R123 and calcein-AM. GF120918 was used as a positive control for inhibition (2 µM for ABCG2 and 1 µM for P-gp), and DMSO (2%) was used as a negative control. An average fluorescence value per 10,000 cells was reported for each sample. Histogram plots were constructed from the mean fluorescence values. IC₅₀ values were subsequently calculated with GraphPad Prism 4.0 using a sigmoidal dose-response model where $Y = \text{bottom} + (\text{top} - \text{bottom}) / (1 + 10^{(\log IC_{50} - X) \times \text{HillSlope}})$.

[¹²⁵I]-IAAP Photoaffinity Cross-Linking Assay. Photoaffinity cross-linking assays were performed as previously described with some modifications.⁶⁰ The substrate [¹²⁵I]-iodoarylazidoprazosin ([¹²⁵I]-IAAP) (specific activity of 2,200 Ci/mmol) was used to photolabel P-gp or ABCG2. Crude Sf9 membranes expressing P-gp (25 µg) or ABCG2 (40 µg) were incubated with either DMSO, GF120918 (10 µM), or increasing concentrations of compounds of interest in assay buffer (50 mM Tris-HCl, pH 7.5, 1% aprotinin, 1 mM DTT, and 2 mM AEBSEF) and [¹²⁵I]-IAAP (3 nM) at room temperature for 10 min protected from light. The samples were illuminated with UV light (365 nm) for 20 min on ice. The samples were separated by SDS-PAGE on a 7.5% Tris-glycine gel. The gel was fixed, dried, and exposed to autoradiography film at -80 °C for 24–48 h. The P-gp or ABCG2 band intensities were quantified using ImageJ to determine the amount of [¹²⁵I]-IAAP photo-cross-linked to P-gp or ABCG2. Values are presented as a percentage of the DMSO control, and an IC₅₀ was calculated using GraphPad Prism 4.0.

DTT Stability. DTT stability studies were performed as described previously with minor modifications.⁴¹ Briefly, Pal dimers (150 µM) were incubated with 10 mM DTT in PBS (pH 7.4) containing the internal standard, benzophenone (25 µM), at 37 °C. DMSO concentrations were kept at 0.75%. At varying time points, aliquots from the reaction were collected and frozen immediately on dry ice. Samples were stored at -80 °C until analytical HPLC analysis as described below. The peak area corresponding to the released monomeric Pal was quantified, and half-lives were obtained by fitting data using GraphPad Prism 4.0. Assays were performed in triplicate.

HPLC Analysis. Samples were thawed and immediately analyzed by reverse phase HPLC using a C18 analytical column (Phenomenex, Torrance, CA) with an eluent consisting of solvent A (acetonitrile and 0.1% TFA) and solvent B (water and 0.1% TFA) with a 30 min gradient of 20–80% A. Flow rate was 1.20 mL/min, and peaks were detected at 280 nm.

Human Plasma Stability. Plasma stability studies were performed as described previously with minor modifications.⁴¹ Pal dimers (120 µM) were incubated in 55% human plasma, 44% PBS (pH 7.4) with a constant DMSO concentration of 0.6% at 37 °C. At varying time point, aliquots were collected and the reaction was halted by the addition of ice cold acetonitrile containing the internal standard, benzophenone (25 µM). The solution was vortexed for 20 s and centrifuged at 13000g for 10 min. The supernatant was collected and stored at -80 °C until HPLC analysis as described above. The peak areas

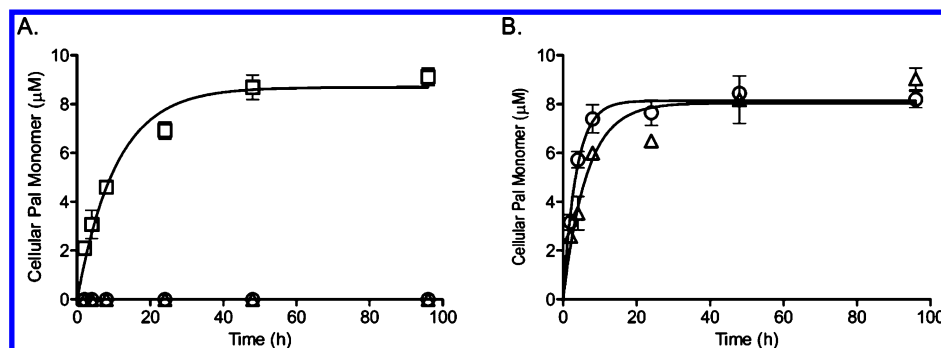


Figure 1. Intracellular accumulation of Pal in cells expressing P-gp or ABCG2. Pal (20 μM) was incubated with MCF-7 cells (\square), MCF-7/DX1 cells overexpressing P-gp (Δ), and MCF-7/FLV1000 cells overexpressing ABCG2 (O) in the absence (DMSO) (A) or presence of the dual inhibitor GF120918 (2.5 μM) (B). At increasing time points, cells were collected, washed, and lysed, the intracellular Pal accumulation was monitored and quantified by analytical HPLC, and the concentration of Pal was calculated from a standard curve. Error bars represent standard deviation from three independent experiments.

corresponding to Pal dimer and released Pal monomer were quantified, and half-lives were calculated by fitting the time-dependent data using GraphPad Prism 4.0. Assays were performed in triplicate.

ATP Hydrolysis Stimulation Assay. Vanadate-sensitive ATP hydrolysis was analyzed in the presence or absence of increasing concentrations of Pal or Pal dimer as described previously.⁶⁰ Briefly, crude membranes (10 μg) from MCF-7/DX1 cells, MCF-7/FLV1000 cells, or Sf9 cells expressing either P-gp or ABCG2 were incubated with DMSO or test compounds in assay buffer (45 mM Tris-HCl, pH 7.5, 5 mM sodium azide, 10 mM MgCl₂, 2 mM EGTA, 1 mM ouabain, and 2 mM DTT) in the presence or absence of 300 μM sodium orthovanadate. The reaction was initiated by the addition of ATP (5 mM final) making the total volume 100 μL and incubated at 37 $^{\circ}\text{C}$ for 20 min. The reaction was terminated with the addition of 100 μL of 5% (w/v) SDS, and the ATPase activity was measured by the colorimetric determination of inorganic phosphate released. A minimum of two assays were performed in duplicate.

ATP Hydrolysis Inhibition Assay. Verapamil (30 μM) and prazosin (40 μM) stimulated ATP hydrolysis was quantified for P-gp and ABCG2 respectively. Samples were prepared as in the stimulation assay in the presence of increasing concentrations of Pal compounds as inhibitors of substrate-stimulated ATPase activity. A minimum of two assays were performed in duplicate.

Cell Assay Toxicity. Cell viability in the presence of increasing concentrations of Pal dimers was analyzed using the colorimetric MTT assay.⁶² MCF-7, MCF-7/DX1, or MCF-7/FLV1000 cells (3,000 cells per well) were plated in a 96-well plate (Costar, Corning Life Sciences, Acton, MA) in 100 μL per well. Following incubation at 37 $^{\circ}\text{C}$ overnight, the medium was replaced with 100 μL of medium containing increasing concentrations of Pal dimer. The DMSO concentration was kept constant at 0.5%. After cells were incubated at 37 $^{\circ}\text{C}$ for 72 h, 20 μL of a 5 mg/mL solution of 3-(4,5-dimethylthiazol-2-yl)-2,5-diphenyltetrazolium bromide (MTT) was added to each well and incubated for an additional 4 h at 37 $^{\circ}\text{C}$. The medium was carefully removed, and the formazan crystals were solubilized in 100 μL of DMSO. The absorbance was read at 590 nm, and the average absorbance for each concentration of dimer was plotted using GraphPad Prism 4.0. IC₅₀ values represent the concentration of dimer leading to 50% cell viability \pm SD.

Pal Accumulation in MCF-7 Cells. Pal accumulation was studied in MCF-7 (parent line), MCF-7/DX1 (P-gp-overexpressing), and MCF-7/FLV1000 (ABCG2-overexpressing) cells as described previously with modifications.^{63,64} Cells were plated (5×10^5 cells/well) in 6-well plates and cultured overnight at 37 $^{\circ}\text{C}$ with 5% CO₂. Culture medium was replaced with medium containing 20 μM Pal. At varying time points, medium was aspirated and wells were washed five times with cold phosphate buffered saline (PBS) (pH 7.4). The plate was incubated for 5 min in ice-cold radioimmunoprecipitation assay (RIPA) buffer (150 mM NaCl, 0.25% sodium deoxycholate, 1% SDS, 20 mM Tris-HCl, pH 7.5), and the cell lysate was collected with a sterile cell scraper. Ice cold acetonitrile containing the internal standard, benzophenone (25 μM), was added, and the lysates were vortexed for 20 s. At the different time points, samples were centrifuged at 13,000g for 10 min and the supernatant was collected and stored at -80°C until HPLC analysis as described above. The peak area corresponding to Pal was quantified and converted to intracellular concentration using a standard curve made up of known concentrations of Pal analyzed under the same HPLC conditions. Monomer concentration was plotted using GraphPad Prism 4.0. Plots represent a minimum of two independent assays.

Pal Accumulation in hCMEC/D3 Cells with Coadministration of ABC Transporter Inhibitors. Pal accumulation in hCMEC/D3 cells was studied as described previously with modifications.^{63,64} Cells were plated (1×10^6 cells/well) in 6-well plates and cultured overnight at 37 $^{\circ}\text{C}$ with 5% CO₂. Culture medium was replaced with medium containing 20 μM Pal plus the inhibitors GF120918 (2.5 μM) or Pal-carbamate (4 μM), and the cells were incubated at 37 $^{\circ}\text{C}$ with 5% CO₂. DMSO was used as the vehicle control. At varying time points, cells and samples were analyzed as described in the Pal accumulation study above. A minimum of two independent assays were performed.

Pal-8SSMe Accumulation and Breakdown in hCMEC/D3 Cells. Cells were seeded (1×10^6 cells/well) in 6-well plates and cultured overnight at 37 $^{\circ}\text{C}$. Culture medium was replaced with medium containing Pal-8SSMe (7.5 μM) and incubated at 37 $^{\circ}\text{C}$ with 5% CO₂. At varying time points, cells were treated as described in the Pal accumulation study. The same conditions were used for HPLC analysis as described above except that a gradient of 10–70% A was used to

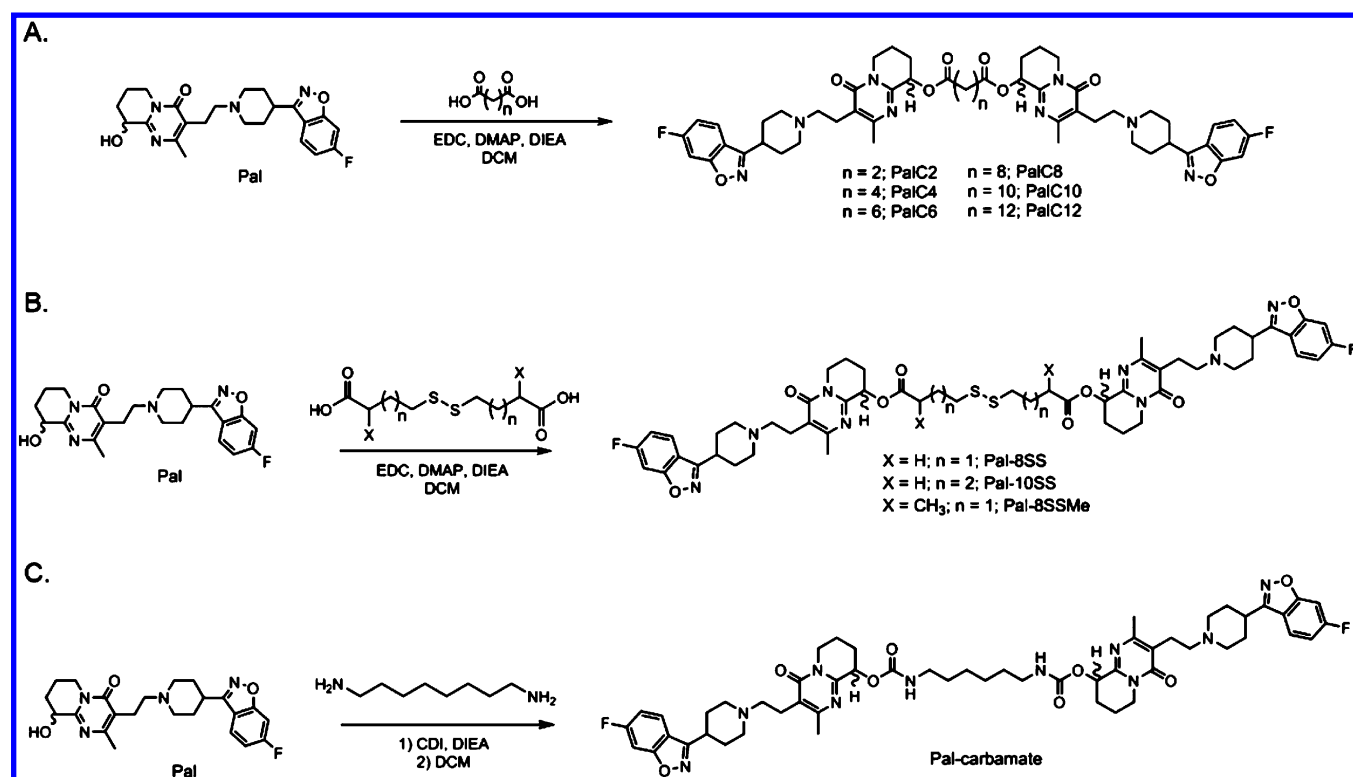


Figure 2. Synthetic scheme for Pal prodrug homodimers. Prodrug Pal dimers were synthesized as described in [Experimental Procedures](#). (A) Dimers were named for the number of methylene (–CH₂–) groups between the ester bonds. (B) Dimers were named by the number of methylene groups and sulfur atoms between the ester bonds. Pal-8SSMe contains two additional methyl groups in the tether alpha to the carbonyl in the ester moiety. (C) Pal-carbamate was synthesized using a diamine tether containing eight carbons. Dimers were purified to >95% by reverse phase HPLC and characterized by analytical HPLC and ESI mass spectrometry.

maximize peak separation with an acetophenone (0.025 mM) standard. Three independent assays were performed.

RESULTS AND DISCUSSION

Paliperidone Is a Substrate for ABCG2 and P-gp. To demonstrate that Pal does not accumulate within MCF-7 cells that overexpress P-gp (MCF-7/DX1) or ABCG2 (MCF-7/FLV1000), we monitored the cellular levels of Pal over time by HPLC. Briefly, cells were incubated with Pal (20 μM) in medium. At the indicated time points, cells were lysed as described in [Experimental Procedures](#) and the supernatant was analyzed by analytical HPLC to quantitate the levels of intracellular Pal. The parental MCF-7 cell line, which does not overexpress an ABC transporter, was used as a control. Pal accumulated to ~8 μM in the parental cells ([Figure 1A](#)). In contrast, Pal did not accumulate to detectable levels in either cell line overexpressing P-gp or ABCG2 ([Figure 1A](#)). GF120918, one of the few reported dual P-gp/ABCG2 inhibitors, was used to probe whether Pal would accumulate in MCF-7/DX1 cells or MCF-7/FLV1000 cells upon inhibition of P-gp or ABCG2 ([Figure 1B](#)). In the presence of GF120918, cellular accumulation of Pal in cells overexpressing either transporter increased dramatically after 10 min as compared to the cells without inhibitor. Furthermore, the overall cellular levels of Pal observed in the presence of GF120918 were comparable to those seen in the parental line ([Figure 1A](#)). These results demonstrate that Pal is transported by both P-gp and ABCG2. These data taken together with the fact that Pal inhibits these transporters at high concentrations^{26,27} suggest

Table 1. Inhibition of P-gp Mediated Calcein-AM Transport and ABCG2-Mediated Mitoxantrone Transport by Pal and Pal Dimers

compound	P-gp IC ₅₀ (μM) ^{a,b}	ABCG2 IC ₅₀ (μM) ^{a,c}
Pal	52.9 ± 3	96 ± 7
PalC2	24.9 ± 0.8	5.8 ± 0.7
PalC4	5.5 ± 0.2	3.9 ± 0.4
PalC6	3.3 ± 0.1	5.5 ± 0.3
PalC8	1.7 ± 0.2	4.6 ± 0.5
PalC10	2.1 ± 0.1	7.2 ± 0.9
PalC12	5.5 ± 0.2	3.9 ± 0.7
Pal-8SS	1.8 ± 0.2	2.2 ± 0.3
Pal-10SS	6.5 ± 0.6	4.9 ± 0.6

^aIC₅₀ values are reported as the concentration of Pal or Pal dimer resulting in half-maximum fluorescence level ± SEM. ^bMCF-7/DX1 cells with 0.5 μM calcein-AM. Calcein-AM accumulation in MCF-7/DX1 cells was quantified in the 96-well plate high throughput assay as described in [Experimental Procedures](#). For each concentration point, the average of total well fluorescence was used to generate a dose response curve. ^cMCF-7/FLV1000 cells with 20 μM mitoxantrone. Mitoxantrone accumulation in MCF-7/FLV1000 cells was quantified using the flow cytometry assay described in [Experimental Procedures](#). For each concentration point, the mean fluorescence of 10,000 cells was used to generate a dose response curve in a minimum of two separate assays.

that bivalent Pal derivatives may be useful as more effective dual P-gp/ABCG2 inhibitors.

Design and Synthesis of Pal Dimers. Pal has been shown to have limited access to the brain most likely due to recognition by the ABC transporters P-gp and ABCG2. These

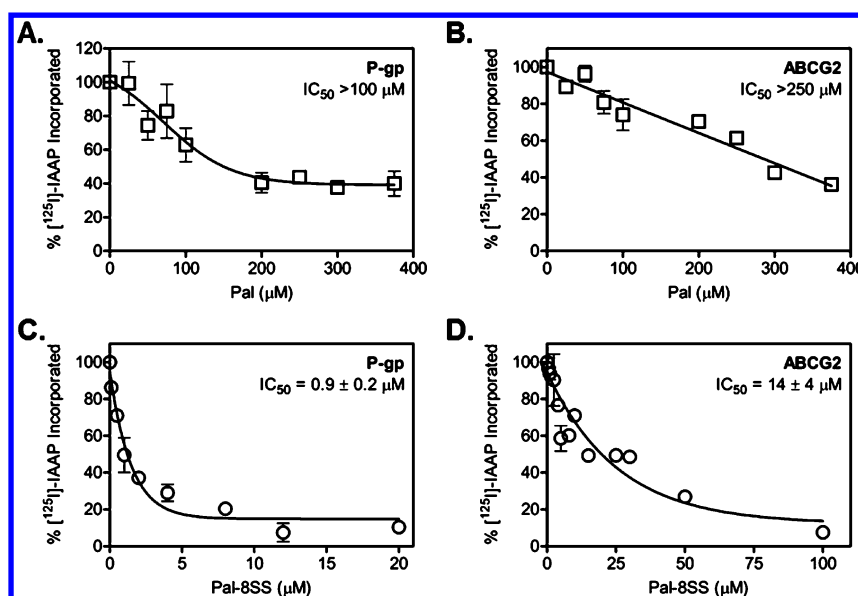


Figure 3. P-gp and ABCG2 drug binding competition photo-cross-linking assay. Crude Sf9 membranes expressing P-gp (25 μg) or ABCG2 (40 μg) were incubated with the substrate [^{125}I]-IAAP in the presence of increasing concentrations of Pal (\square) or Pal-8SS (\circ) for 10 min. Samples were photo-cross-linked at 365 nm on ice for 20 min and separated by SDS-PAGE. [^{125}I]-IAAP labeling was visualized by autoradiography and quantified using ImageJ (NIH) as described in [Experimental Procedures](#). Values were plotted as a percentage of the DMSO control, and IC_{50} values were calculated using GraphPad Prism 4.0.

Table 2. Stability Analysis of Pal Dimers *in Vitro*^a

compound	10 mM DTT: $t_{1/2}$ (h)	55% human plasma: $t_{1/2}$ (h)
Pal-8SS	2.9 \pm 0.6	0.5 \pm 0.1
Pal-8SSMe	2.2 \pm 0.5	11.4 \pm 2.8

^aPal dimers (150 μM) were incubated with 10 mM DTT or 55% human plasma at 37 $^{\circ}\text{C}$. Half-lives represent the time at which half of total reversion to monomer was observed by HPLC.

Table 3. Inhibition of P-gp and ABCG2 Mediated Substrate Transport by Pal and the Pal Dimers Pal-8SS and Pal-8SSMe

compound	P-gp IC_{50} (μM) in MCF-7/DX1 cells with 0.5 μM calcein-AM	P-gp IC_{50} (μM) in MCF-7/DX1 cells with 0.5 $\mu\text{g}/\text{mL}$ RI23	ABCG2 IC_{50} (μM) in MCF-7/FLV1000 cells with 20 μM mitoxantrone
Pal	52.9 \pm 3	>150	96 \pm 7
Pal-8SS	1.9 \pm 0.2	2.6 \pm 0.2	2.2 \pm 0.3
Pal-8SSMe	3.6 \pm 0.5	4.0 \pm 0.3	2.8 \pm 0.5

^a IC_{50} values are reported as the concentration of Pal or Pal dimer resulting in half-maximum fluorescence level \pm SEM using the flow cytometry assay described in [Experimental Procedures](#).

transporters have been shown to have substrate and inhibitor overlap and are both proposed to have spatially distinct binding sites for their transport substrates.^{23,25,28–38} We have previously reported the advantage of developing P-gp inhibitors using bivalency and degradable linkers.^{40–43} In an effort to obtain a prodrug dual inhibitor of P-gp and ABCG2, a library of Pal dimers was designed. Pal has a free secondary alcohol that was used to link two Pal monomers via ester moieties using tethers of varying lengths ([Figures 2A and 2B](#)). The original library consisted of eight Pal dimers with tethers ranging from two to 12 methylene units in an effort to probe the efficacy of inhibition as a function of tether length ([Figure 2A](#)). Two disulfide containing tethers were also designed in which the two central methylene units of each tether in PalC8 and PalC10 were replaced with a disulfide bond ([Figure 2B](#)). This disulfide

bond was engineered within the tethers to provide a reductive route for regenerating monomeric Pal within cells. In this way, the dual inhibitors would also serve as prodrugs of Pal due to the traceless nature of these tethers.^{41,65–67} These tethers have been previously used to link other agents in cell-based experiments with no adverse effects observed.^{41,65,66,68}

One challenge with having ester bonds linking the tether to Pal is the potential for facile breakdown by esterases in plasma. To circumvent this potential difficulty, two additional dimeric agents were designed: one containing an additional methyl group alpha to each carbonyl of the tether ([Figure 2B](#)) and one containing a carbamate ([Figure 2C](#)). The former was designed to sterically block esterase attack at the carbonyl of the tether^{41,69,70} whereas the carbamate should not appreciably act as a substrate for esterases.

The ester and disulfide containing Pal homodimers were synthesized by reacting Pal with the appropriate dicarboxylic acid tethers activated with 1-ethyl-3-(3-(dimethylamino)propyl)carbodiimide (EDC) ([Figures 2A and 2B](#)). The carbamate containing dimer was synthesized by treating Pal with 1,1'-carbonyldiimidazole followed by 1,8-diaminooctane ([Figure 2C](#)). Dimers were purified to homogeneity by reverse phase HPLC and characterized by electrospray ionization mass spectrometry.

Pal Dimers Inhibit Cellular Efflux by P-gp and ABCG2.

Pal homodimers were evaluated as inhibitors of P-gp and ABCG2 in MCF7-DX1 and MCF-7/FLV1000 cells, respectively. To test for inhibition of P-gp export activity, we measured the accumulation of calcein in a rapid cell based assay with monomeric Pal as a control ([Table 1](#)).⁶¹ Cells are incubated with the P-gp substrate calcein-AM. If not effluxed, calcein-AM that enters cells is rapidly converted to the fluorescent compound calcein inside cells by cellular esterases. For ABCG2, we measured the accumulation of one of its fluorescent substrates, mitoxantrone, in the presence and absence of inhibitor using flow cytometry and Pal monomer as a control. For both assays, mean cellular fluorescence was

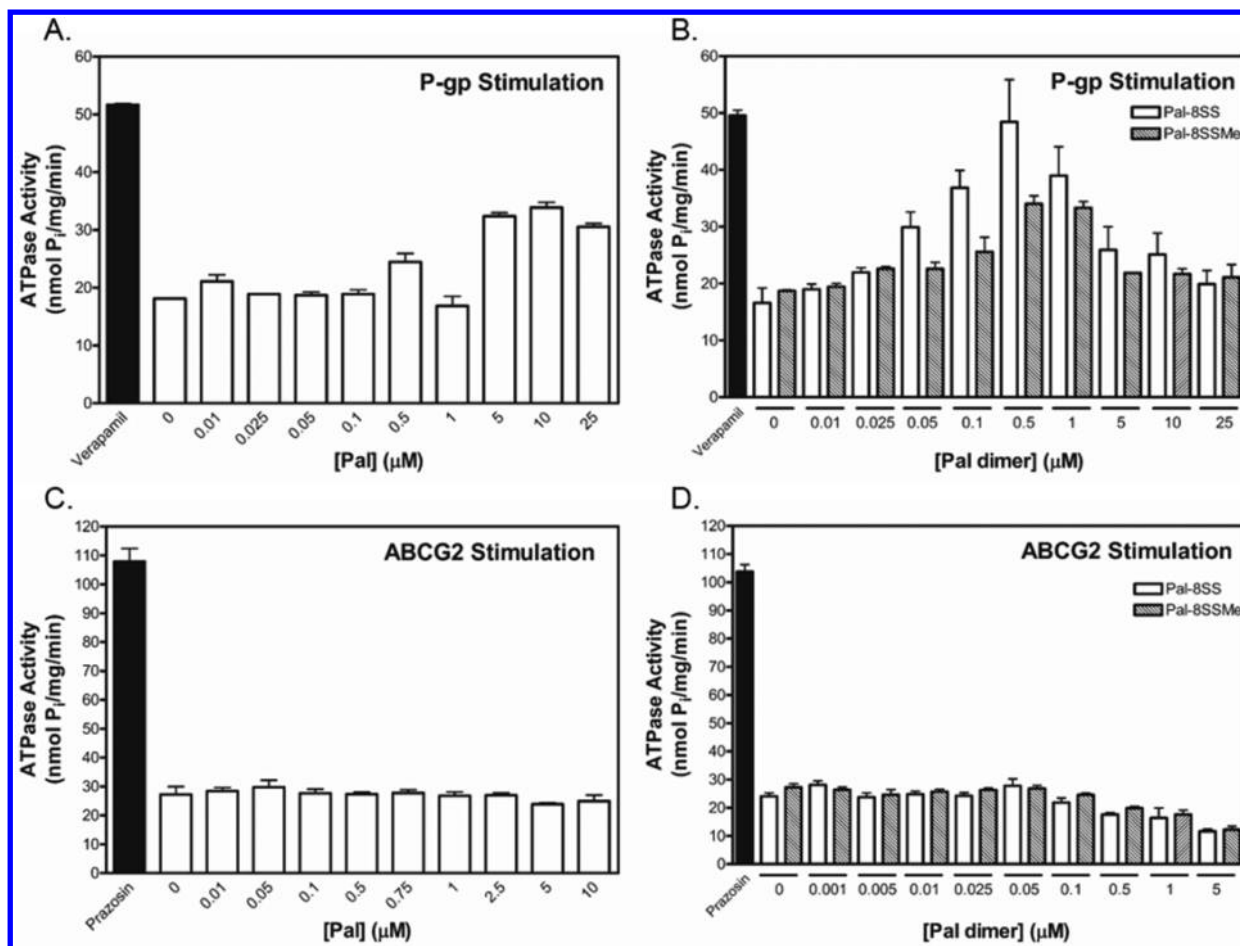


Figure 4. Stimulation of P-gp and ABCG2 ATPase activity by Pal, Pal-8SS, and Pal-8SSMe. Crude membrane vesicles from Sf9 or MCF-7 cells overexpressing P-gp or ABCG2 (10 μg) were incubated with Pal or Pal dimer for 20 min at 37 °C. Verapamil (30 μM) and prazosin (40 μM) were used as control stimulating drugs for P-gp and ABCG2 respectively. ATPase activity was determined by quantifying the release of inorganic phosphate spectrophotometrically as described in [Experimental Procedures](#). A minimum of two assays were performed in duplicate for each compound.

plotted and IC₅₀ values were calculated for each compound (Table 1).

Screening the library for inhibition of substrate transport by P-gp revealed that all of the dimers were more effective inhibitors than the Pal monomer (Table 1). Dimers with tethers containing more than two methylene units provided low micromolar inhibition (Table 1). PalC2 was a less effective inhibitor of P-gp mediated calcein-AM transport with an IC₅₀ of ~25 μM. Optimum activity was obtained with PalC8 and PalC10 with IC₅₀ values of ~2 μM. PalC8 was 3.2- and 1.9-fold more potent than PalC4 and PalC6, respectively, and 3.2-fold more potent than PalC12. The introduction of a disulfide in the tether (Pal-8SS) had no effect on inhibitory potency when compared to PalC8, but potency was reduced 3-fold when incorporated into the C10 series.

Similar to P-gp, all of the dimers were more potent inhibitors of ABCG2 transport than monomeric Pal (Table 1). Unlike P-gp, however, ABCG2 showed little variance in potency across the different tether lengths, with the most effective inhibitor Pal-8SS displaying 2–3-fold greater efficacy as compared to the other tether lengths (Table 1). In P-gp, the binding sites are located within a single monomeric protein whereas in ABCG2 two subunits come together to form the binding sites. This difference could allow ABCG2 to have increased flexibility, allowing it to accommodate different tether lengths. Further

studies were continued using the Pal dimer, Pal-8SS in the interest of pursuing the best inhibitor as well as using the reductive strategy for regenerating Pal inside cells.

Pal-8SS Competed for Substrate Binding in Both P-gp and ABCG2. The Pal dimers were designed to interact directly with the binding site(s) in P-gp and ABCG2, with the goal of creating competitive binding inhibitors. To evaluate binding, we performed photoaffinity cross-linking assays with the dual P-gp/ABCG2 substrate, [¹²⁵I]-IAAP, a prazosin analogue (Figure 3). Crude membrane preparations expressing either P-gp or ABCG2 were incubated in the presence of increasing concentrations of Pal or Pal-8SS. Samples were photo-cross-linked and subsequently subjected to SDS-PAGE. [¹²⁵I]-IAAP labeled proteins were visualized using autoradiography and quantified densitometrically. The decrease in photolabeled protein, which is indicative of competition for the binding site, was used to generate an IC₅₀ for each compound. The Pal monomer did not completely eliminate [¹²⁵I]-IAAP labeling up to 400 μM for both P-gp and ABCG2 (Figures 3A and 3B, Figure S.1). In striking contrast, Pal-8SS competed for substrate binding with IC₅₀ values of 0.9 ± 0.2 μM and 14 ± 4 μM with the P-gp and ABCG2 membrane preparations, respectively (Figures 3C and 3D, Figure S.1). Since [¹²⁵I]-IAAP is known to interact directly with the transmembrane binding sites,⁷¹ these results support the hypothesis that Pal-8SS is in fact inhibiting

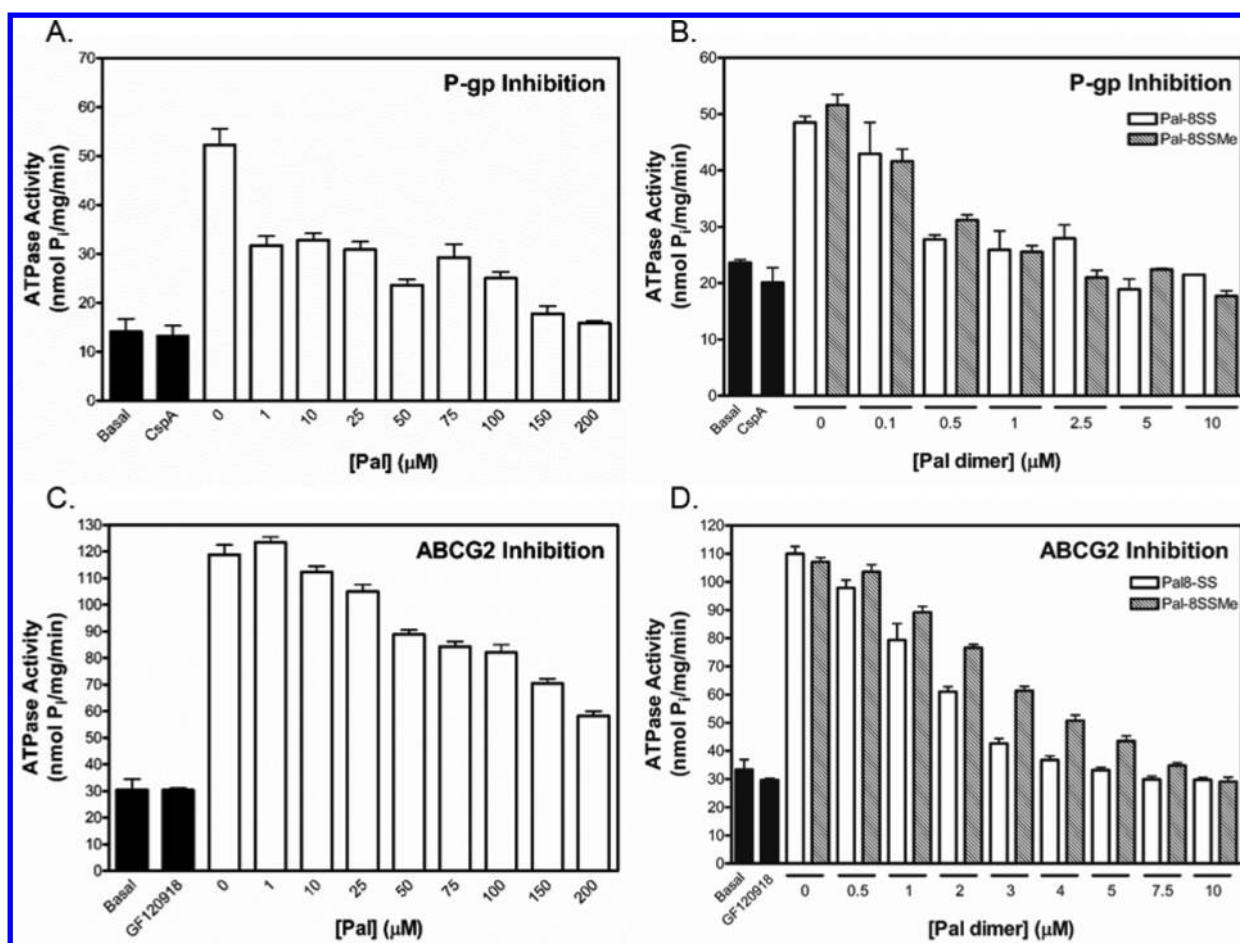


Figure 5. Inhibition of substrate-stimulated ATPase activity of P-gp and ABCG2 by Pal, Pal-8SS, and Pal-8SSMe. Drug-stimulated ATP hydrolysis was quantified for P-gp and ABCG2 using verapamil (30 μM) and prazosin (40 μM) respectively. Samples were prepared as in the stimulation assay but with the addition of increasing concentrations of Pal, Pal-8SS, or Pal-8SSMe as inhibitors. A minimum of two assays were performed in duplicate.

Table 4. Inhibition of Substrate-Stimulated ATP Hydrolysis Activity of P-gp and ABCG2 by Pal and Pal Dimers

compound	P-gp verapamil-stimulated ATPase activity IC_{50} (μM)	ABCG2 prazosin-stimulated ATPase activity IC_{50} (μM)
Pal	>25	>25
Pal-8SS	2.4 \pm 1.5	2.4 \pm 0.3
Pal-8SSMe	1.1 \pm 0.4	4.0 \pm 0.2

P-gp and ABCG2 by interacting with the substrate binding sites in both of these ABC transporters.

Pal-8SS Generated Monomer under Reductive Conditions and in Human Plasma, Necessitating Tether Redesign. With the addition of a disulfide bond into the tether, Pal-8SS was designed to revert to the therapeutic monomer in the reducing environment of the cell through an addition/elimination process. However, to effectively reach the brain intact, the dimer needs to be relatively stable to the esterases present in human plasma. To evaluate breakdown under both conditions, Pal-8SS was incubated with either 55% human plasma or 10 mM DTT and subjected to analytical HPLC. Reversion to monomer was monitored and quantified over time, and a half-life ($t_{1/2}$) was calculated (Table 2). Pal-8SS demonstrated a $t_{1/2}$ of ~ 3 h in the presence of DTT but was readily hydrolyzed in the presence of human plasma (Table 2). To increase stability to esterases, we introduced a hindering

methyl group alpha to each carbonyl within the tether, generating Pal-8SSMe. Pal-8SSMe demonstrated a similar susceptibility to DTT as Pal-8SS but with a >20-fold improved stability to human plasma. The ability of the hindering methyl groups to provide increased stability to plasma esterases demonstrates that the tether can be engineered to provide the desired reversion characteristics. We designed these dimeric compounds with disulfide bonds in the tether. Once inside the reducing environment of cells, the disulfide bond will be broken and the tether will undergo intramolecular addition and elimination reactions to release the therapeutic monomer, a process which is independent of esterase activity.

Addition of Hindering Methyl Groups Does Not Alter Inhibitory Potency. Pal-8SSMe was assayed as a P-gp and ABCG2 inhibitor to verify that the changes made in tether design did not sacrifice inhibitory potency. Using flow cytometry, efflux of calcein-AM and R123 for P-gp in MCF-7/DX1 cells and mitoxantrone for ABCG2 in MCF-7/FLV1000 cells was quantified. Pal-8SSMe inhibited fluorescent substrate accumulation with low micromolar IC_{50} values for all three fluorescent substrates (Table 3). For P-gp, Pal-8SSMe was 1.5–1.9-fold less active than Pal-8SS but the two compounds were approximately equipotent for ABCG2. These results allowed us to pursue further studies with both Pal-8SS and Pal-8SSMe as potent dual inhibitors of P-gp and ABCG2.

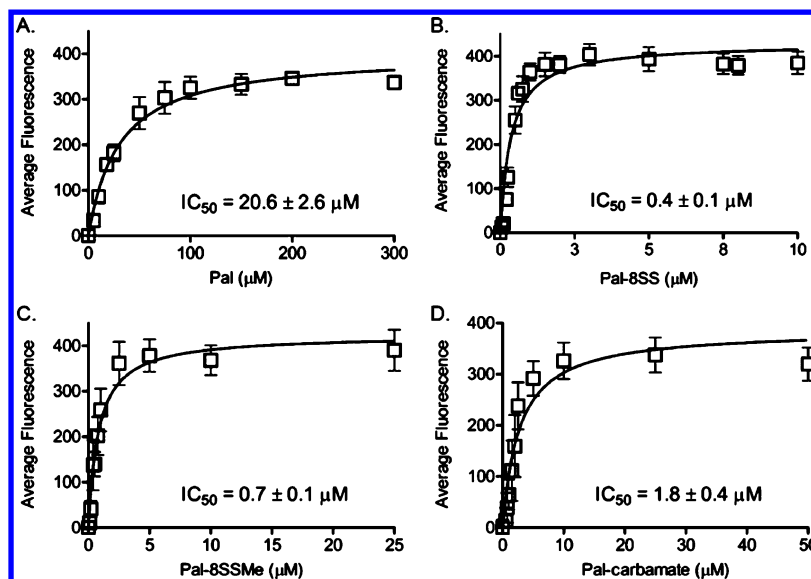


Figure 6. Inhibition of P-gp transport in immortalized human hCMEC/D3 cells derived from the BBB. IC_{50} values \pm SEM for the inhibition of P-gp transport of R123 ($0.5 \mu\text{g/mL}$) by Pal (A), Pal-8SS (B), Pal-8SSMe (C), and Pal-carbamate (D) in immortalized human hCMEC/D3 cells. Each curve represents the mean of two independent experiments \pm SEM.

Table 5. MTT Assay for Cellular Toxicity of Pal Dimers

cell line	IC_{50} (μM) ^a		
	Pal-8SS	Pal-8SSMe	Pal-carbamate
MCF-7/DX1 (P-gp)	47.7 ± 1.6	20.9 ± 2.6	N/D
MCF-7/FLV1000 (ABCG2)	36.2 ± 2.4	26.4 ± 1.8	N/D
hCMEC/D3 (BBB)	18.0 ± 1.8	14.4 ± 0.7	8.0 ± 0.4

^a IC_{50} values represent the concentration at which the dimer caused 50% of cell death using a 72 h MTT assay.

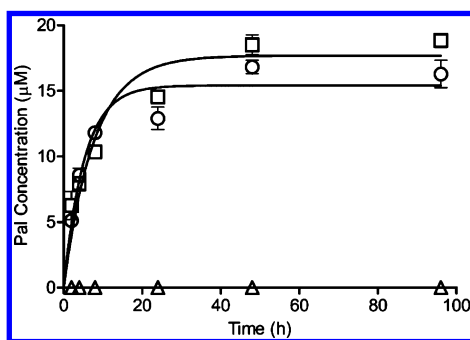


Figure 7. Pal accumulation in immortalized human hCMEC/D3 cells derived from the BBB. hCMEC/D3 cells were coincubated with Pal ($20 \mu\text{M}$) and either Pal-carbamate ($4 \mu\text{M}$) (\square), GF120918 ($2.5 \mu\text{M}$) (\circ), or DMSO as a control (Δ). At increasing time points, cells were collected, washed, and lysed, the intracellular Pal accumulation was quantified by analytical HPLC as described in [Experimental Procedures](#), and the concentration of Pal was calculated from a standard curve. Error bars represent standard deviation from three independent experiments.

Pal-8SS and Pal-8SSMe Inhibit the Substrate-Stimulated ATPase Activity of Both P-gp and ABCG2. Many substrates and inhibitors of ABC transporters stimulate the basal ATPase activities of the transporters and/or inhibit their drug-stimulated ATPase activities, thereby indicating that these compounds physically interact with the transporters.^{23,72} To determine if Pal and the Pal dimers Pal-8SS and Pal-8SSMe interact with P-gp and ABCG2, we performed ATPase activity

assays using crude membrane preparations from cells over-expressing either transporter.

The Pal dimers Pal-8SS and Pal-8SSMe stimulated the basal activity of P-gp at a concentration 10–20-fold lower than the Pal monomer (Figures 4A and 4B). Furthermore, Pal-8SS and Pal-8SSMe inhibited the verapamil-stimulated ATPase activity of P-gp with IC_{50} values also at least 10–20-fold lower than that of the Pal monomer (Figures 5A and 5B and Table 4). In contrast to P-gp, neither Pal nor the dimers stimulated the basal ATPase activity of ABCG2 (Figures 4C and 4D). However, all three compounds inhibited the prazosin-stimulated ATPase activity of ABCG2 with varying potency (Table 4, Figures 5C and 5D). The Pal-8SS and Pal 8SSMe dimers inhibited with low micromolar IC_{50} values that were at least 10–20-fold lower than that of the Pal monomer (Figures 5C and 5D and Table 4). Similar results to these observed for ABCG2 were previously reported for both ABCG2 and P-gp with compounds such as the flavonoids, tyrosine kinase inhibitors, tariquidar, and gomisin A.^{23,24,73–75} These compounds also did not stimulate the ATPase activity of P-gp or ABCG2, but significantly inhibited the drug-stimulated activity. These data suggest the possibility that the dimers are also low affinity for substrates for P-gp but not necessarily ABCG2.

Taken together, these data demonstrate that Pal and the Pal-8SS and Pal-8SSMe dimers interact with both P-gp and ABCG2 to affect either the basal or substrate-stimulated ATPase activities of the transporters. The data also suggest that the dimers interact with P-gp and ABCG2 with higher affinity than the Pal monomer. This hypothesis is further supported by our substrate photo-cross-linking data demonstrating that Pal-8SS competed much more effectively for substrate binding than the Pal monomer to both P-gp and ABCG2 (Figure 3 and Figure S.1). Lastly, the dimers were also much more effective at inhibiting the cellular efflux of fluorescent transport substrates than the monomer (Tables 1 and 3).

Pal Dimers Inhibit P-gp Activity in Cells Derived from the Human BBB. With evidence that Pal dimers could potentially inhibit both P-gp and ABCG2 in overexpressing cell lines, we sought a more relevant model of the BBB that could

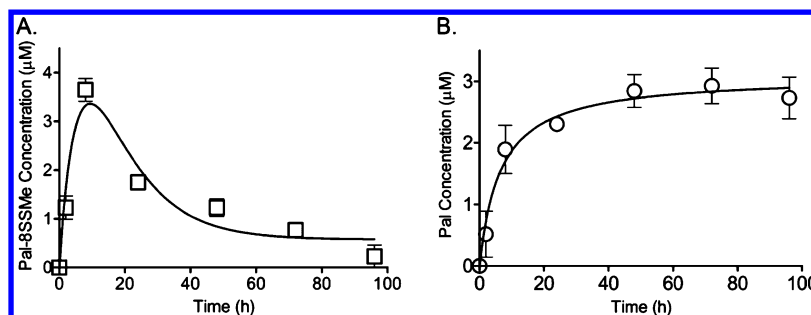


Figure 8. Pal-8SSMe accumulation and reversion in hCMEC/D3 cells derived from the BBB. hCMEC/D3 cells were incubated with Pal-8SSMe (7.5 μM). At varying time points, cells were collected, washed, and lysed. Pal-8SSMe (A) and Pal (B) were monitored by analytical HPLC. Pal and Pal-8SSMe concentrations were calculated using a standard curve from monomer and dimer peak areas and plotted using GraphPad Prism 4.0. Error bars represent the standard deviation from three independent experiments.

be used with our flow cytometry inhibition assay. To this end, we employed the hCMEC/D3 cell line derived from the human BBB⁵⁷ and evaluated the accumulation of the substrate R123 in the presence of increasing concentration of Pal, Pal-8SS, and Pal-8SSMe (Figure 6). Both of the dimers Pal-8SS and Pal-8SSMe inhibited R123 accumulation with sub-micromolar IC_{50} values (Figures 6B and 6C). These results indicate that Pal-8SS and Pal-8SSMe can increase cellular substrate accumulation in cells modeling the BBB by inhibiting P-gp. Immunoblot and flow cytometry experiments of hCMEC/D3 lysates and cells did not show the presence of ABCG2 in this cell line (data not shown); therefore we could only evaluate for P-gp inhibition.

Pal Dimers Are Not Toxic to Cells at Concentrations Used in Experiments. Pal-8SS, Pal-8SSMe, and a non-hydrolyzable dimer Pal-carbamate were assessed for their cytotoxicity using an MTT assay with MCF-7/DX1, MCF-7/FLV1000, and hCMEC/D3 cells. IC_{50} values were determined after incubation of each of the dimers with cells for 72h (Table 5). All of the IC_{50} values were at least 2-fold higher than the highest concentration used in any of our cell-based transport assays. The IC_{50} for the Pal monomer was $>75 \mu\text{M}$ in hCMEC/D3 cells and $>500 \mu\text{M}$ in MCF-7/DX1 and MCF-7/FLV1000 cells (data not shown). These data suggest that cells were viable during the course of the inhibition and accumulation experiments described. As we advance these compounds further into models, we will first perform a PK/PD study to fully evaluate toxicity.

Coincubation with a Nonhydrolyzable Pal Dimer Allows for Accumulation of Pal in BBB Cells. One feasible approach to increasing the brain access of Pal is to coadminister the dimeric prodrugs and monomeric Pal. To this end, hCMEC/D3 cells were incubated with Pal in the presence of a nonhydrolyzable Pal dimer, Pal-carbamate, or the control inhibitor GF120918 (Figure 7). A nonhydrolyzable Pal dimer was used so we would only measure the accumulation of exogenously added monomeric Pal. The cellular concentration of Pal was determined using analytical HPLC of cell lysates over time in hCMEC/D3 cells. Pal-carbamate accumulated but did not break down into Pal monomer over a 72 h time course (data not shown). In the absence of inhibitor, Pal did not accumulate in the BBB cells (Figure 7). However, when coincubated with either Pal-carbamate or GF120918, Pal accumulated to maximal concentration in approximately 24 h. These data demonstrate that coadministration of Pal with Pal dimers can significantly increase the concentration of the active Pal agent within BBB cells. It should be noted that there is the

potential for a 3-fold higher concentration of Pal within the BBB cells using this coadministration approach.

Pal Dimers Accumulate and Break Down in BBB Cells.

In addition to being useful for coadministration to increase the levels of monomeric Pal within cells, we had designed the tethers of Pal-8SS and Pal-8SSMe to break down in the reducing environment of cells, thereby producing an extra bolus of Pal within cells. To test this design, Pal-8SSMe was incubated alone with hCMEC/D3 cells and, at varying time points, the cells were lysed and levels of Pal and Pal-8SSMe were monitored by analytical HPLC. Pal-8SSMe reached maximal accumulation at 8 h with a subsequent drop in dimer concentration at longer time points (Figure 8A). As these levels dropped, there was a concomitant increase in the concentration of Pal within cells, with maximal levels observed at approximately 24 h (Figure 8B). These results indicate that Pal-8SSMe, administered alone, is capable of both preventing drug efflux and reverting to its original monomeric therapeutic form, thus acting as a prodrug.

■ ASSOCIATED CONTENT

Supporting Information

The Supporting Information is available free of charge on the ACS Publications website at DOI: 10.1021/acs.molpharmaceut.6b01044.

Autoradiographs of [¹²⁵I]-IAAP competition assay (PDF)

■ AUTHOR INFORMATION

Corresponding Authors

*Department of Chemistry, Purdue University, West Lafayette, IN 47907. Tel: (765) 494-7322. E-mail: Hrycyna@purdue.edu.

*Department of Chemistry, Purdue University, West Lafayette, IN 47907. Tel: (765) 494-0135. E-mail: chml@purdue.edu.

ORCID

Christine A. Hrycyna: 0000-0001-9881-2063

Author Contributions

C.A.H., J.C., and K.B. conceived and coordinated the study. K.B., C.A.H., and J.C. wrote the paper. K.B. performed the experiments in Figures 2–6. A.L. performed the experiments in Figures 1, 2, 7, and 8. K.B. performed the experiments in Tables 1, 3, 4, and 5. K.B. prepared the figures and tables. All authors reviewed the results and approved the final version of the manuscript.

Notes

The authors declare no competing financial interest.

ACKNOWLEDGMENTS

This work was supported by NIH Grant R21EY018481 from NEI/NIH.

ABBREVIATIONS USED

ABC, ATP-binding cassette; AEBSF, 4-(2-aminoethyl)-benzenesulfonyl fluoride hydrochloride; BBB, blood–brain barrier; BME, basal medium Eagle; BV, baculovirus; calcein-AM, calcein acetoxymethyl ester; CNS, central nervous system; CspA, cyclosporin A; DIEA, *N,N*-diisopropylethylamine; DTT, dithiothreitol; EDC, *N*-(3-(dimethylamino)propyl)-*N*-ethylcarbodiimide; EGTA, ethylene glycol tetraacetic acid; FBS, fetal bovine serum; [¹²⁵I]-IAAP, [¹²⁵I]-iodoarylazidoprazosin; MTT, 3-(4,5-dimethylthiazol-2-yl)-2,5-diphenyltetrazolium bromide; Pal, paliperidone; PBS, phosphate buffered saline; P-gp, P-glycoprotein; R123, rhodamine 123; RIPA, radioimmunoprecipitation assay buffer; TFA, trifluoroacetic acid; TKI, tyrosine kinase inhibitor; WHO, World Health Organization

REFERENCES

- (1) Ustun, T. B.; Rehm, J.; Chatterji, S.; Saxena, S.; Trotter, R.; Room, R.; Bickenbach, J. Multiple-informant ranking of the disabling effects of different health conditions in 14 countries. WHO/NIH Joint Project CAR Study Group. *Lancet* **1999**, *354* (9173), 111–115.
- (2) Raggi, M. A.; Mandrioli, R.; Sabbioni, C.; Pucci, V. Atypical antipsychotics: pharmacokinetics, therapeutic drug monitoring and pharmacological interactions. *Curr. Med. Chem.* **2004**, *11* (3), 279–296.
- (3) Taub, A. L.; Kolotilin, A.; Gibbons, R. S.; Berndt, E. R. *The Diversity of Concentrated Prescribing Behavior: an Application to Antipsychotics*; NBER Working Paper No. w16823; National Bureau of Economic Research: 2011.
- (4) Rui, Q.; Wang, Y.; Liang, S.; Liu, Y.; Wu, Y.; Wu, Q.; Nuamah, I.; Gopal, S. Relapse prevention study of paliperidone extended-release tablets in Chinese patients with schizophrenia. *Prog. Neuro-Psychopharmacol. Biol. Psychiatry* **2014**, *53*, 45–53.
- (5) Wang, S. M.; Han, C.; Lee, S. J.; Patkar, A. A.; Pae, C. U.; Fleischacker, W. W. Paliperidone: a review of clinical trial data and clinical implications. *Clin. Drug Invest.* **2012**, *32* (8), 497–512.
- (6) Hitchcock, S. A. Blood-brain barrier permeability considerations for CNS-targeted compound library design. *Curr. Opin. Chem. Biol.* **2008**, *12* (3), 318–323.
- (7) Pardridge, W. M. Blood-brain barrier delivery. *Drug Discovery Today* **2007**, *12* (1–2), 54–61.
- (8) Weiss, N.; Miller, F.; Cazaubon, S.; Couraud, P. O. The blood-brain barrier in brain homeostasis and neurological diseases. *Biochim. Biophys. Acta, Biomembr.* **2009**, *1788* (4), 842–857.
- (9) De Hert, M.; Detraux, J.; van Winkel, R.; Yu, W. P.; Correll, C. U. Metabolic and cardiovascular adverse effects associated with antipsychotic drugs. *Nat. Rev. Endocrinol.* **2012**, *8* (2), 114–126.
- (10) Ucock, A.; Gaebel, W. Side effects of atypical antipsychotics: a brief overview. *World Psychiatry* **2008**, *7* (1), 58–62.
- (11) Cordon-Cardo, C.; O'Brien, J. P.; Casals, D.; Rittman-Grauer, L.; Biedler, J. L.; Melamed, M. R.; Bertino, J. R. Multidrug-resistance gene (P-glycoprotein) is expressed by endothelial cells at blood-brain barrier sites. *Proc. Natl. Acad. Sci. U. S. A.* **1989**, *86* (2), 695–698.
- (12) Loscher, W.; Potschka, H. Drug resistance in brain diseases and the role of drug efflux transporters. *Nat. Rev. Neurosci.* **2005**, *6* (8), 591–602.
- (13) O'Brien, F. E.; Dinan, T. G.; Griffin, B. T.; Cryan, J. F. Interactions between antidepressants and P-glycoprotein at the blood-brain barrier: clinical significance of in vitro and in vivo findings. *Br. J. Pharmacol.* **2012**, *165* (2), 289–312.
- (14) Schinkel, A. H. P-Glycoprotein, a gatekeeper in the blood-brain barrier. *Adv. Drug Delivery Rev.* **1999**, *36* (2–3), 179–194.

- (15) Wang, J. S.; Zhu, H. J.; Markowitz, J. S.; Donovan, J. L.; DeVane, C. L. Evaluation of antipsychotic drugs as inhibitors of multidrug resistance transporter P-glycoprotein. *Psychopharmacology (Berl)* **2006**, *187* (4), 415–423.
- (16) Honjo, Y.; Hrycyna, C. A.; Yan, Q. W.; Medina-Perez, W. Y.; Robey, R. W.; van de Laar, A.; Litman, T.; Dean, M.; Bates, S. E. Acquired mutations in the MXR/BCRP/ABCP gene alter substrate specificity in MXR/BCRP/ABCP-overexpressing cells. *Cancer Res.* **2001**, *61* (18), 6635–6639.
- (17) Robey, R. W.; Medina-Perez, W. Y.; Nishiyama, K.; Lahusen, T.; Miyake, K.; Litman, T.; Senderowicz, A. M.; Ross, D. D.; Bates, S. E. Overexpression of the ATP-binding cassette half-transporter, ABCG2 (MXR/BCRP/ABCP1), in flavopiridol-resistant human breast cancer cells. *Clin. Cancer Res.* **2001**, *7* (1), 145–152.
- (18) Lagas, J. S.; van Waterschoot, R. A.; Sparidans, R. W.; Wagenaar, E.; Beijnen, J. H.; Schinkel, A. H. Breast cancer resistance protein and P-glycoprotein limit sorafenib brain accumulation. *Mol. Cancer Ther.* **2010**, *9* (2), 319–326.
- (19) Matsson, P.; Pedersen, J. M.; Norinder, U.; Bergstrom, C. A. S.; Artursson, P. Identification of Novel Specific and General Inhibitors of the Three Major Human ATP-Binding Cassette Transporters P-gp, BCRP and MRP2 Among Registered Drugs. *Pharm. Res.* **2009**, *26* (8), 1816–1831.
- (20) Feng, B.; Mills, J. B.; Davidson, R. E.; Mireles, R. J.; Janiszewski, J. S.; Troutman, M. D.; de Moraes, S. M. In vitro P-glycoprotein assays to predict the in vivo interactions of P-glycoprotein with drugs in the central nervous system. *Drug Metabolism and Disposition: The Biological Fate of Chemicals* **2008**, *36* (2), 268–275.
- (21) Doran, A.; Obach, R. S.; Smith, B. J.; Hosea, N. A.; Becker, S.; Callegari, E.; Chen, C.; Chen, X.; Choo, E.; Cianfrogna, J.; Cox, L. M.; Gibbs, J. P.; Gibbs, M. A.; Hatch, H.; Hop, C. E.; Kasman, I. N.; Laperle, J.; Liu, J.; Liu, X.; Logman, M.; Maclin, D.; Nedza, F. M.; Nelson, F.; Olson, E.; Rahematpura, S.; Raunig, D.; Rogers, S.; Schmidt, K.; Spracklin, D. K.; Szcw, M.; Troutman, M.; Tseng, E.; Tu, M.; Van Deusen, J. W.; Venkatakrishnan, K.; Walens, G.; Wang, E. Q.; Wong, D.; Yasgar, A. S.; Zhang, C. The impact of P-glycoprotein on the disposition of drugs targeted for indications of the central nervous system: evaluation using the MDRIA/1B knockout mouse model. *Drug Metab. Dispos.* **2005**, *33* (1), 165–174.
- (22) Wang, J. S.; Ruan, Y.; Taylor, R. M.; Donovan, J. L.; Markowitz, J. S.; De Vane, C. L. The brain entry of risperidone and 9-hydroxyrisperidone is greatly limited by P-glycoprotein. *Int. J. Neuropsychopharmacol.* **1999**, *7* (4), 415–419.
- (23) Ambudkar, S. V.; Dey, S.; Hrycyna, C. A.; Ramachandra, M.; Pastan, I.; Gottesman, M. M. Biochemical, cellular, and pharmacological aspects of the multidrug transporter. *Annu. Rev. Pharmacol. Toxicol.* **1999**, *39*, 361–398.
- (24) Kannan, P.; Telu, S.; Shukla, S.; Ambudkar, S. V.; Pike, V. W.; Halldin, C.; Gottesman, M. M.; Innis, R. B.; Hall, M. D. The "Specific" P-Glycoprotein Inhibitor Tariquidar Is Also a Substrate and an Inhibitor for Breast Cancer Resistance Protein (BCRP/ABCG2). *ACS Chem. Neurosci.* **2011**, *2* (2), 82–89.
- (25) Sharom, F. J.; Liu, R.; Romsicki, Y.; Lu, P. Insights into the structure and substrate interactions of the P-glycoprotein multidrug transporter from spectroscopic studies. *Biochim. Biophys. Acta, Biomembr.* **1999**, *1461* (2), 327–45.
- (26) Zhu, H. J.; Wang, J. S.; Markowitz, J. S.; Donovan, J. L.; Gibson, B. B.; DeVane, C. L. Risperidone and paliperidone inhibit P-glycoprotein activity in vitro. *Neuropsychopharmacology* **2007**, *32* (4), 757–764.
- (27) Wang, J. S.; Zhu, H. J.; Markowitz, J. S.; Donovan, J. L.; Yuan, H. J.; Devane, C. L. Antipsychotic drugs inhibit the function of breast cancer resistance protein. *Basic Clin. Pharmacol. Toxicol.* **2008**, *103* (4), 336–341.
- (28) Aller, S. G.; Yu, J.; Ward, A.; Weng, Y.; Chittaboina, S.; Zhuo, R.; Harrell, P. M.; Trinh, Y. T.; Zhang, Q.; Urbatsch, I. L.; Chang, G. Structure of P-glycoprotein reveals a molecular basis for poly-specific drug binding. *Science* **2009**, *323* (5922), 1718–1722.

- (29) Chufan, E. E.; Kapoor, K.; Sim, H. M.; Singh, S.; Talele, T. T.; Durell, S. R.; Ambudkar, S. V. Multiple transport-active binding sites are available for a single substrate on human P-glycoprotein (ABCB1). *PLoS One* **2013**, *8* (12), e82463.
- (30) Chufan, E. E.; Sim, H.-M.; Ambudkar, S. V. Chapter Three - Molecular Basis of the Polyspecificity of P-glycoprotein (ABCB1): Recent Biochemical and Structural Studies. *Adv. Cancer Res.* **2015**, *125*, 71–96.
- (31) Clark, R.; Kerr, I. D.; Callaghan, R. Multiple drugbinding sites on the R482G isoform of the ABCG2 transporter. *Br. J. Pharmacol.* **2006**, *149* (5), 506–515.
- (32) Dey, S.; Ramachandra, M.; Pastan, I.; Gottesman, M. M.; Ambudkar, S. V. Evidence for two nonidentical drug-interaction sites in the human P-glycoprotein. *Proc. Natl. Acad. Sci. U. S. A.* **1997**, *94*, 10594–10599.
- (33) Giri, N.; Agarwal, S.; Shaik, N.; Pan, G.; Chen, Y.; Elmquist, W. F. Substrate-dependent breast cancer resistance protein (Bcrp1/Abcg2)-mediated interactions: consideration of multiple binding sites in vitro assay design. *Drug metabolism and Disposition: The Biological Fate of Chemicals* **2009**, *37* (3), 560–570.
- (34) Loo, T. W.; Bartlett, M. C.; Clarke, D. M. Simultaneous binding of two different drugs in the binding pocket of the human multidrug resistance P-glycoprotein. *J. Biol. Chem.* **2003**, *278* (41), 39706–39710.
- (35) Martin, C.; Berridge, G.; Higgins, C. F.; Mistry, P.; Charlton, P.; Callaghan, R. Communication between multiple drug binding sites on P-glycoprotein. *Mol. Pharmacol.* **2000**, *58* (3), 624–632.
- (36) Shapiro, A. B.; Ling, V. Positively cooperative sites for drug transport by P-glycoprotein with distinct drug specificities. *Eur. J. Biochem.* **1997**, *250* (1), 130–137.
- (37) Shapiro, A. B.; Ling, V. Extraction of Hoechst 33342 from the cytoplasmic leaflet of the plasma membrane by P-glycoprotein. *Eur. J. Biochem.* **1997**, *250* (1), 122–129.
- (38) Shapiro, A. B.; Ling, V. Transport of LDS-751 from the cytoplasmic leaflet of the plasma membrane by the rhodamine-123-selective site of P-glycoprotein. *Eur. J. Biochem.* **1998**, *254* (1), 181–188.
- (39) Jin, M. S.; Oldham, M. L.; Zhang, Q.; Chen, J. Crystal structure of the multidrug transporter P-glycoprotein from *Caenorhabditis elegans*. *Nature* **2012**, *490* (7421), 566–569.
- (40) Emmert, D.; Campos, C. R.; Ward, D.; Lu, P.; Namanja, H. A.; Bohn, K.; Miller, D. S.; Sharom, F. J.; Chmielewski, J.; Hrycyna, C. A. Reversible dimers of the atypical antipsychotic quetiapine inhibit P-glycoprotein-mediated efflux in vitro with increased binding affinity and in situ at the blood-brain barrier. *ACS Chem. Neurosci.* **2014**, *5* (4), 305–317.
- (41) Namanja, H. A.; Emmert, D.; Davis, D. A.; Campos, C.; Miller, D. S.; Hrycyna, C. A.; Chmielewski, J. Toward eradicating HIV reservoirs in the brain: inhibiting P-glycoprotein at the blood-brain barrier with prodrug abacavir dimers. *J. Am. Chem. Soc.* **2012**, *134* (6), 2976–2980.
- (42) Pires, M. M.; Emmert, D.; Hrycyna, C. A.; Chmielewski, J. Inhibition of P-glycoprotein-mediated paclitaxel resistance by reversibly linked quinine homodimers. *Mol. Pharmacol.* **2009**, *75* (1), 92–100.
- (43) Pires, M. M.; Hrycyna, C. A.; Chmielewski, J. Bivalent probes of the human multidrug transporter P-glycoprotein. *Biochemistry* **2006**, *45* (38), 11695–11702.
- (44) Sauna, Z. E.; Andrus, M. B.; Turner, T. M.; Ambudkar, S. V. Biochemical basis of polyvalency as a strategy for enhancing the efficacy of P-glycoprotein (ABCB1) modulators: stipiamide homodimers separated with defined-length spacers reverse drug efflux with greater efficacy. *Biochemistry* **2004**, *43* (8), 2262–2271.
- (45) Chan, K. F.; Zhao, Y.; Burkett, B. A.; Wong, I. L.; Chow, L. M.; Chan, T. H. Flavonoid dimers as bivalent modulators for P-glycoprotein-based multidrug resistance: synthetic apigenin homodimers linked with defined-length poly(ethylene glycol) spacers increase drug retention and enhance chemosensitivity in resistant cancer cells. *J. Med. Chem.* **2006**, *49* (23), 6742–59.
- (46) Chan, K. F.; Zhao, Y.; Chow, T. W.; Yan, C. S.; Ma, D. L.; Burkett, B. A.; Wong, I. L.; Chow, L. M.; Chan, T. H. Flavonoid dimers as bivalent modulators for p-glycoprotein-based multidrug resistance: structure-activity relationships. *ChemMedChem* **2009**, *4* (4), 594–614.
- (47) Wong, I. L.; Chan, K. F.; Burkett, B. A.; Zhao, Y.; Chai, Y.; Sun, H.; Chan, T. H.; Chow, L. M. Flavonoid dimers as bivalent modulators for pentamidine and sodium stibogluconate resistance in leishmania. *Antimicrob. Agents Chemother.* **2007**, *51* (3), 930–940.
- (48) Gu, X.; Ren, Z.; Peng, H.; Peng, S.; Zhang, Y. Bifendate-chalcone hybrids: a new class of potential dual inhibitors of P-glycoprotein and breast cancer resistance protein. *Biochem. Biophys. Res. Commun.* **2014**, *455* (3–4), 318–322.
- (49) de Bruin, M.; Miyake, K.; Litman, T.; Robey, R.; Bates, S. E. Reversal of resistance by GF120918 in cell lines expressing the ABC half-transporter, MXR. *Cancer Lett.* **1999**, *146* (2), 117–126.
- (50) Kruijtzter, C. M. F.; Beijnen, J. H.; Rosing, H.; ten Bokkel Huinink, W. W.; Schot, M.; Jewell, R. C.; Paul, E. M.; Schellens, J. H. M. Increased oral bioavailability of topotecan in combination with the breast cancer resistance protein and P-glycoprotein inhibitor GF120918. *J. Clin. Oncol.* **2002**, *20* (13), 2943–2950.
- (51) Minderman, H.; O'Loughlin, K. L.; Pendyala, L.; Baer, M. R. VX-710 (biricodar) increases drug retention and enhances chemosensitivity in resistant cells overexpressing P-glycoprotein, multidrug resistance protein, and breast cancer resistance protein. *Clin. Cancer Res.* **2004**, *10* (5), 1826–1834.
- (52) Shukla, S.; Robey, R. W.; Bates, S. E.; Ambudkar, S. V. Sunitinib (Sutent, SU11248), a small-molecule receptor tyrosine kinase inhibitor, blocks function of the ATP-binding cassette (ABC) transporters P-glycoprotein (ABCB1) and ABCG2. *Drug Metabolism and Disposition: The Biological Fate of Chemicals* **2009**, *37* (2), 359–365.
- (53) Danieli, B.; Giardini, A.; Lesma, G.; Passarella, D.; Peretto, B.; Sacchetti, A.; Silvani, A.; Pratesi, G.; Zunino, F. Thiocolchicine-podophyllotoxin conjugates: Dynamic libraries based on disulfide exchange reaction. *J. Org. Chem.* **2006**, *71* (7), 2848–2853.
- (54) Lu, Y. L.; Tanasova, M.; Borhan, B.; Reid, G. E. Ionic Reagent for Controlling the Gas-Phase Fragmentation Reactions of Cross-Linked Peptides. *Anal. Chem.* **2008**, *80* (23), 9279–9287.
- (55) Soule, H. D.; Vazquez, J.; Long, A.; Albert, S.; Brennan, M. Human Cell Line from a Pleural Effusion Derived from a Breast Carcinoma. *J. Natl. Cancer Inst.* **1973**, *51* (5), 1409–1416.
- (56) Fairchild, C. R.; Ivy, S. P.; Kao-Shan, C. S.; Whang-Peng, J.; Rosen, N.; Israel, M. A.; Melera, P. W.; Cowan, K. H.; Goldsmith, M. E. Isolation of amplified and overexpressed DNA sequences from adriamycin-resistant human breast cancer cells. *Cancer Res.* **1987**, *47* (19), 5141–5148.
- (57) Weksler, B. B.; Subileau, E. A.; Perriere, N.; Charneau, P.; Holloway, K.; Leveque, M.; Tricoire-Leignel, H.; Nicotra, A.; Bourdoulous, S.; Turowski, P.; Male, D. K.; Roux, F.; Greenwood, J.; Romero, I. A.; Couraud, P. O. Blood-brain barrier-specific properties of a human adult brain endothelial cell line. *FASEB J.* **2005**, *19* (13), 1872–1874.
- (58) Germann, U. A.; Willingham, M. C.; Pastan, I.; Gottesman, M. M. Expression of the human multidrug transporter in insect cells by a recombinant baculovirus. *Biochemistry* **1990**, *29*, 2295–2303.
- (59) Ozvegy, C.; Litman, T.; Szakacs, G.; Nagy, Z.; Bates, S.; Varadi, A.; Sarkadi, B. Functional characterization of the human multidrug transporter, ABCG2, expressed in insect cells. *Biochem. Biophys. Res. Commun.* **2001**, *285* (1), 111–117.
- (60) Hrycyna, C. A.; Ramachandra, M.; Pastan, I.; Gottesman, M. M. Functional expression of human P-glycoprotein from plasmids using vaccinia virus-bacteriophage T7 RNA polymerase system. *Methods Enzymol.* **1998**, *292*, 456–473.
- (61) Bauer, B.; Miller, D. S.; Fricker, G. Compound profiling for P-glycoprotein at the blood-brain barrier using a microplate screening system. *Pharm. Res.* **2003**, *20* (8), 1170–1176.

(62) Mosmann, T. Rapid colorimetric assay for cellular growth and survival: application to proliferation and cytotoxicity assays. *J. Immunol. Methods* **1983**, *65* (1–2), 55–63.

(63) Maltese, A.; Maugeri, F.; Drago, F.; Bucolo, C. Simple determination of riluzole in rat brain by high-performance liquid chromatography and spectrophotometric detection. *J. Chromatogr. B: Anal. Technol. Biomed. Life Sci.* **2005**, *817* (2), 331–334.

(64) Milane, A.; Fernandez, C.; Vautier, S.; Bensimon, G.; Meininger, V.; Farinotti, R. Minocycline and riluzole brain disposition: interactions with p-glycoprotein at the blood-brain barrier. *J. Neurochem.* **2007**, *103* (1), 164–173.

(65) Henne, W. A.; Doorneweerd, D. D.; Hilgenbrink, A. R.; Kularatne, S. A.; Low, P. S. Synthesis and activity of a folate peptide camptothecin prodrug. *Bioorg. Med. Chem. Lett.* **2006**, *16* (20), 5350–5355.

(66) Jones, L. R.; Goun, E. A.; Shinde, R.; Rothbard, J. B.; Contag, C. H.; Wender, P. A. Releasable luciferin-transporter conjugates: tools for the real-time analysis of cellular uptake and release. *J. Am. Chem. Soc.* **2006**, *128* (20), 6526–6527.

(67) El Alaoui, A.; Schmidt, F.; Amessou, M.; Sarr, M.; Decaudin, D.; Florent, J. C.; Johannes, L. Shiga toxin-mediated retrograde delivery of a topoisomerase I inhibitor prodrug. *Angew. Chem., Int. Ed.* **2007**, *46* (34), 6469–6472.

(68) Brezden, A.; Mohamed, M. F.; Nepal, M.; Harwood, J. S.; Kuriakose, J.; Seleem, M. N.; Chmielewski, J. Dual Targeting of Intracellular Pathogenic Bacteria with a Cleavable Conjugate of Kanamycin and an Antibacterial Cell-Penetrating Peptide. *J. Am. Chem. Soc.* **2016**, *138* (34), 10945–10949.

(69) Stinchcomb, A. L.; Paliwal, A.; Dua, R.; Imoto, H.; Woodard, R. W.; Flynn, G. L. Permeation of buprenorphine and its 3-alkyl-ester prodrugs through human skin. *Pharm. Res.* **1996**, *13* (10), 1519–1523.

(70) Wagner, J.; Grill, H.; Henschler, D. Prodrugs of etilefrine: synthesis and evaluation of 3'-(O-acyl) derivatives. *J. Pharm. Sci.* **1980**, *69* (12), 1423–1427.

(71) Isenberg, B.; Thole, H.; Tummler, B.; Demmer, A. Identification and localization of three photobinding sites of iodoarylazidoprazosin in hamster P-glycoprotein. *Eur. J. Biochem.* **2001**, *268* (9), 2629–2634.

(72) Boulton, D. W.; DeVane, C. L.; Liston, H. L.; Markowitz, J. S. In vitro P-glycoprotein affinity for atypical and conventional antipsychotics. *Life Sci.* **2002**, *71* (2), 163–199.

(73) Wan, C. K.; Zhu, G. Y.; Shen, X. L.; Chattopadhyay, A.; Dey, S.; Fong, W. F. Gomisin A alters substrate interaction and reverses P-glycoprotein-mediated multidrug resistance in HepG2-DR cells. *Biochem. Pharmacol.* **2006**, *72* (7), 824–837.

(74) Zhang, S. H.; Morris, M. E. Effects of the flavonoids biochanin A, morin, phloretin, and silymarin on P-glycoprotein-mediated transport. *J. Pharmacol. Exp. Ther.* **2003**, *304* (3), 1258–1267.

(75) Ozvegy-Laczka, C.; Hegedus, T.; Varady, G.; Ujhelly, O.; Schuetz, J. D.; Varadi, A.; Keri, G.; Orfi, L.; Nemet, K.; Sarkadi, B. High-affinity interaction of tyrosine kinase inhibitors with the ABCG2 multidrug transporter. *Mol. Pharmacol.* **2004**, *65* (6), 1485–1495.